SANDIA REPORT
SAND2011-8848
Unlimited Release
Printed October 2011

Initial Operating Experience of the La Ola 1.2-MW Photovoltaic System

Jay Johnson, Benjamin Schenkman, Abraham Ellis, Jimmy Quiroz, and Carl Lenox

Prepared by
Sandia National Laboratories
Albuquerque, New Mexico 87185 and Livermore, California 94550

Sandia National Laboratories is a multi-program laboratory managed and operated by Sandia Corporation, a wholly owned subsidiary of Lockheed Martin Corporation, for the U.S. Department of Energy's National Nuclear Security Administration under contract DE-AC04-94AL85000.

Issued by Sandia National Laboratories, operated for the United ***S***tates Department of Energy by Sandia Corporation.

Available to DOE and DOE contractors from
U.S. Department of Energy
Office of Scientific and Technical Information
P.O. Box 62
Oak Ridge, TN 37831

Telephone: (865) 576-8401
Facsimile: (865) 576-5728
E-Mail: reports@adonis.osti.gov
Online ordering: http://www.osti.gov/bridge

Available to the public from
U.S. Department of Commerce
National Technical Information Service
5285 Port Royal Rd.
Springfield, VA 22161

Telephone: (800) 553-6847
Facsimile: (703) 605-6900
E-Mail: orders@ntis.fedworld.gov
Online order: http://www.ntis.gov/help/ordermethods.asp?loc=7-4-0#online

SAND2011-8848
Unlimited Release
Printed October 2011

Initial Operating Experience of the 12-MW La Ola Photovoltaic System

Jay Johnson, Benjamin Schenkman,
Abraham Ellis, and Jimmy Quiroz
Sandia National Laboratories
P.O. Box 5800
Albuquerque, New Mexico 87185-MS1321

Carl Lenox
SunPower Corporation
1414 Harbour Way South
Richmond, CA 94804

Abstract

The 1.2-MW La Ola photovoltaic (PV) power plant in Lanai, Hawaii, has been in operation since December 2009. The host system is a small island microgrid with peak load of 5 MW. Simulations conducted as part of the interconnection study concluded that unmitigated PV output ramps had the potential to negatively affect system frequency. Based on that study, the PV system was initially allowed to operate with output power limited to 50% of nameplate to reduce the potential for frequency instability due to PV variability. Based on the analysis of historical voltage, frequency, and power output data at 50% output level, the PV system has not significantly affected grid performance. However, it should be noted that the impact of PV variability on active and reactive power output of the nearby diesel generators was not evaluated. In summer 2011, an energy storage system was installed to counteract high ramp rates and allow the PV system to operate at rated output. The energy storage system was not fully operational at the time this report was written; therefore, analysis results do not address system performance with the battery system in place.

ACKNOWLEDGMENTS

This work was funded by the U.S. Department of Energy Solar Energy Technologies Program and Department of Energy Office of Electricity. This work is part of a Cooperative Research and Development Agreement (CRADA) with SunPower Corporation. SunPower and Castle & Cooke facilitated deployment of instrumentation and data acquisition.

CONTENTS

FIGURES

TABLES

NOMENCLATURE

AC	alternating current
CDF	cumulative distribution function
DC	direct current
GH	global horizontal
Hz	hertz
kW	kilowatt
MECO	Maui Electric Company
MPP	maximum power point
MW	megawatt
PCC	point of common coupling (grid interconnect)
POA	plane of array
pu	per unit
PV	photovoltaic
RMS	root-mean-square
SNL	Sandia National Laboratories

1. INTRODUCTION

The La Ola 1.2-MW photovoltaic (PV) power plant consists of 12 independently tracking SunPower PV arrays, each connected to a SatCon inverter. This system is owned and operated by Castle & Cooke and is located on the Hawaiian island of Lanai. The host system is a small island microgrid operated by Maui Electric Company (MECO). Simulations conducted as part of the interconnection study[1] concluded that unmitigated PV output ramps had the potential to negatively affect system frequency. Therefore, the interconnection agreement required an energy storage system to mitigate the possibility of system frequency impacts due to high PV output ramping; however, the system was allowed to operate initially with output limited to 50% of nameplate AC rating (600 kW) until the energy storage system was installed. The energy storage system was installed in summer 2011. The energy storage system is designed to limit net output ramp rate to 360 kW/min and thus prevent the possibility of excessive voltage and frequency deviations. At the time this report was written, the storage was not fully operational; therefore, analysis results do not address system performance with the battery system in place.

The PV power plant and host power system is shown in Figure 1. There are a total of eight diesel generators at the Miko generating station, two 2.2 MW and six 1 MW. These diesel generators have historically provided all the electrical power to Lanai's 5-MW peak load. When operating at full output, the PV plant will supply approximately 10% of Lanai's annual energy demand and significantly reduced diesel fuel consumption.

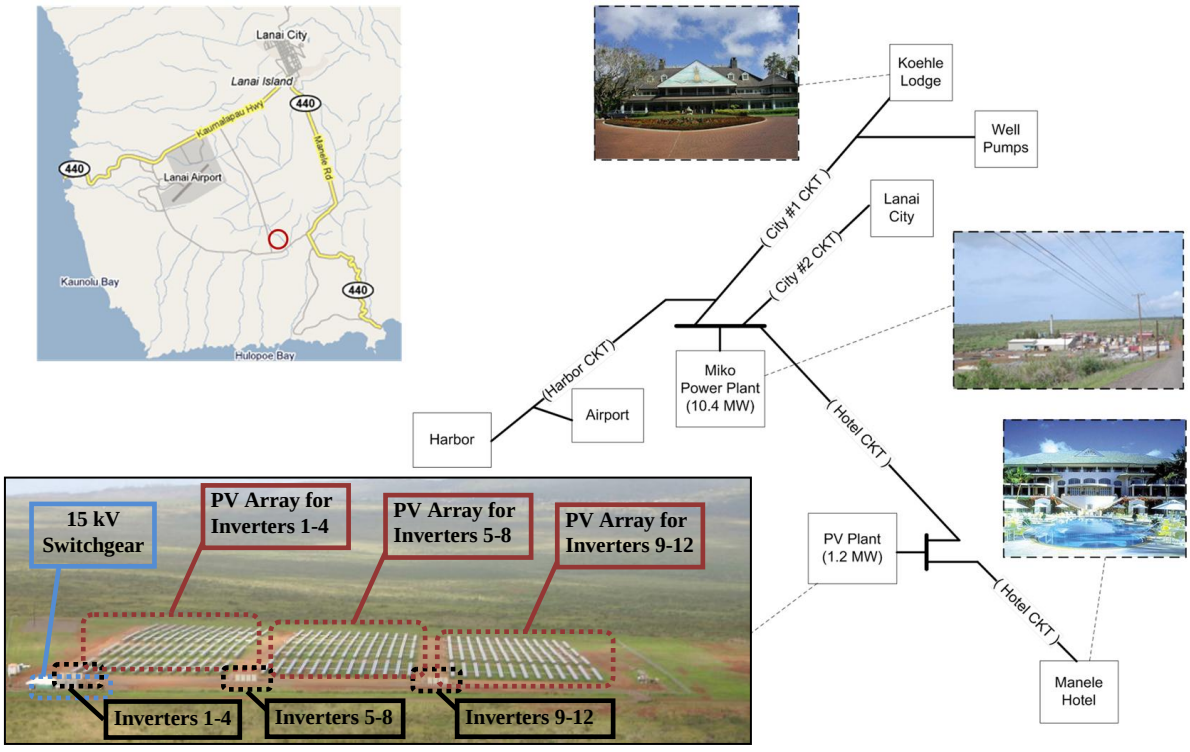

Figure 1. Lanai PV plant and distribution system.

[1] KEMA, Inc., Lanai PV Interconnect Requirements Study: System Impact Study, June 5, 2008, Interconnection Customer: SunPower, KEMA, Inc., Raleigh, NC, USA, 26707.

The PV system integrator, SunPower, has been collecting data at 1-second resolution for the PV power plant, which includes AC and DC electrical measurements at the array, total active/reactive power, and system frequency. The data acquisition system also logs weather data such as plane of array (POA) irradiance, global horizontal (GH) irradiance, module/ambient temperature, and wind speed.[2] Sandia National Laboratories (SNL) and SunPower collaborated to deploy a first-of-a-kind irradiance sensor network at the site, which contributed to better understanding of PV output variability and modeling.[3,4] Data collected at the site is transmitted to SNL near real-time for analysis.

[2] R. Johnson, L. Johnson, L. Nelson, C. Lenox, and J. Stein, Methods of integrating a high penetration photovoltaic power plant into a micro grid, *Photovoltaic Specialists Conference (PVSC), 2010 35th IEEE*, pp. 289-294, June 20-25, 2010, doi: 10.1109/PVSC.2010.5615866.

[3] A. Longhetto, A., G. Elisei, et al., Effect of, correlations in time and spatial extent on performance of very large solar conversion systems, Solar Energy 43(2), pp. 77-84, 1989.

[4] C.W. Hansen, J.S. Stein, and A. Ellis, *Simulation of 1-Minute Power Output from Utility-Scale Photovoltaic Generation Systems*, SAND2011-5529, Sandia National Laboratories, Albuquerque, NM, 2011.

2. IRRADIANCE AND PV POWER VARIABILITY

2.1 Irradiance Characteristics

Solar resource short-term variability on Lanai is high compared to other locations from the standpoint that most days are partly cloudy. The irradiance patterns can be seen in Figure 2.

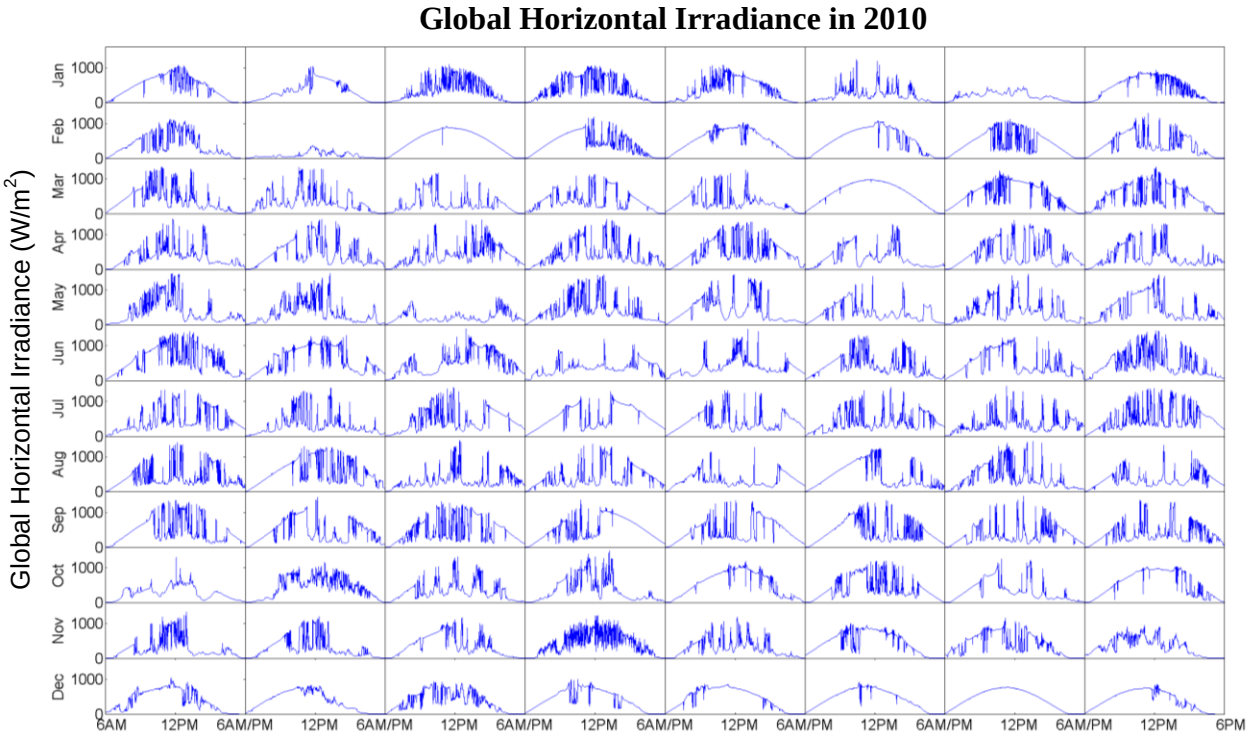

Figure 2. Global horizontal irradiance from one sensor. Data is shown for 8 days at the beginning of each month in 2010.

In 2010, SNL deployed an irradiance sensor network consisting of 12 POA sensors within the PV array.[5] Data from the sensor network is being used to conduct research on spatial and temporal correlation between irradiance and PV plant output, and this topic has been covered in several publications.[6] A basic conclusion is that the uncurtailed output power is proportional to the spatial average POA irradiance over the PV array footprint, and that short-time variability is reduced with the PV array footprint. Figure 3 shows the cumulative distribution functions (CDFs) of the mean irradiance (spatial average of all 12 POA sensors in the array) and the single irradiance sensor that produced the data shown in Figure 3. It can be clearly seen that the spatial average irradiance (mean irradiance) has less variability and fewer large ramp rates than the single sensor.

---

[5] S. Kuszmaul, A. Ellis, et al., Lanai High-Density Irradiance Sensor Network for Characterizing Solar Resource Variability of MW-Scale PV System, *35th IEEE PVSC*, Honolulu, HI, 2010.

[6] A. Mills, M. Ahlstrom, M. Brower, A. Ellis, R. George, T. Hoff, B. Kroposki, C. Lenox, N. Miller, J. Stein, and Y. Wan., *Understanding Variability and Uncertainty of Photovoltaics for Integration with the Electric Power System*, LBNL-2855E, December 2009.

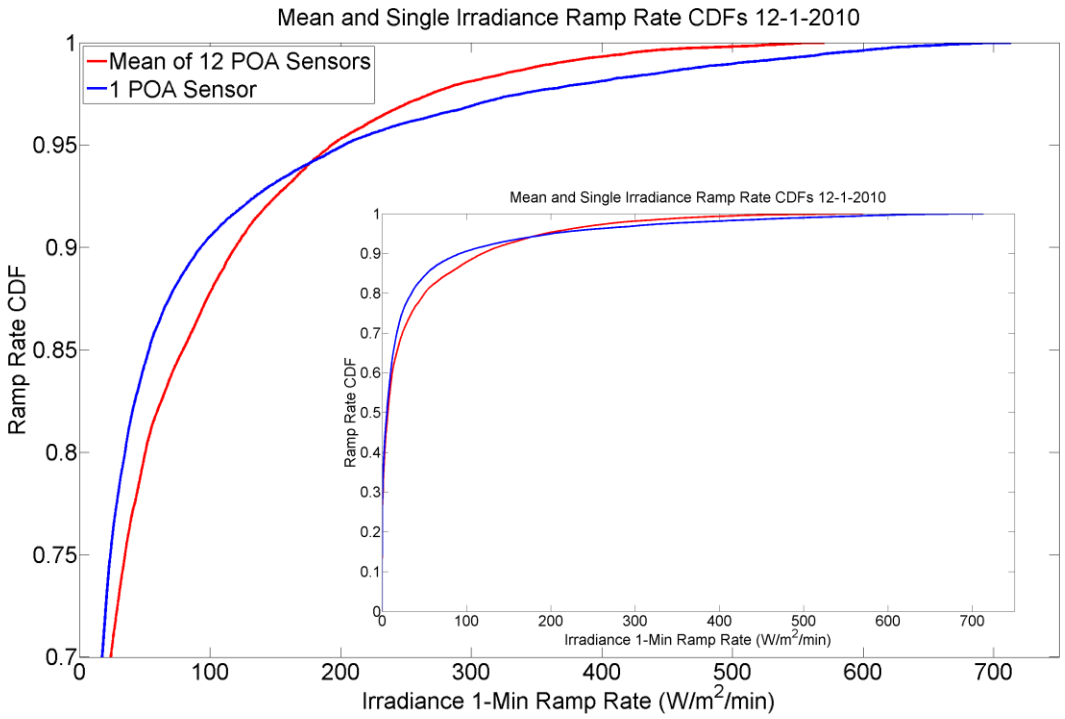

Figure 3. CDFs of the mean irradiance and single irradiance sensor on December 12, 2010.

As described above, the system has been operating with output limited to 600 kW as a way to mitigate the potential for frequency impacts. Reduction in power output is accomplished by configuring the inverter controls to operate away from the PV array maximum power point (MPP) when the available PV power reaches a certain level below their rating. The effect of this control action is shown in Figure 4. In this operating mode, as shown in Section 2.3, the maximum 1-minute output ramp rates are reduced by a factor of approximately 2.

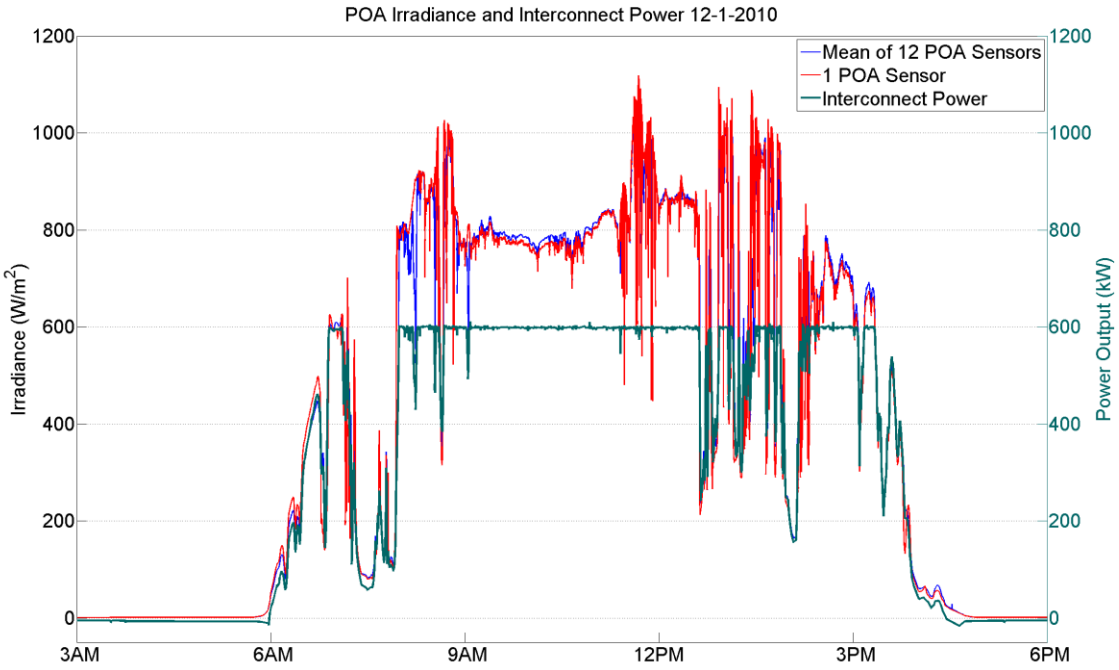

Figure 4. Average irradiance from 12 POA sensors compared to one POA sensor and the interconnect power.

2.2 PV Output Ramp Rates

Using 1-second data, the PV system output ramp rate statistics were derived for the system limited to 50% of rated output, or 600 kW.

An example of ramp rates for two days in December 2010 is shown in Figure 5. The 1-minute ramp rates are shown in the bottom half of the figure. As shown in the figure, clear-weather morning and afternoon ramps are small compared to ramp rates due to irradiance variability. The ramp rates are a function of the daily solar cycle and tracking system. In comparison, ramp rates due to partly cloudy conditions are much higher, often over 200 kW/min. Figure 6 shows the ramp rates for nine selected 1-minute periods. Each ramp rate (red curve) connects two points indicated by the markers (●, □, **x**). For this sample data, the clear-sky ramp rates during the morning sunrise were about 12 kW/min on average, but can be as high as 28 kW/min, while the maximum ramp rate due to irradiance variability was 376 kW/min.

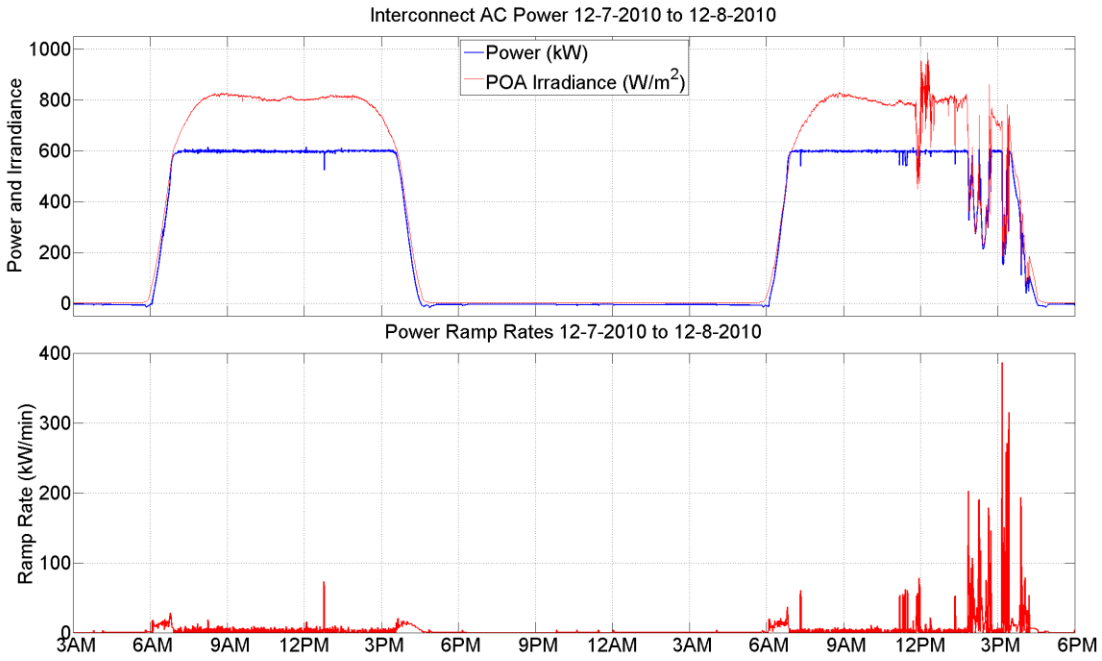

Figure 5. 1-minute morning and evening ramp rates compared to ramp rates from cloud cover.

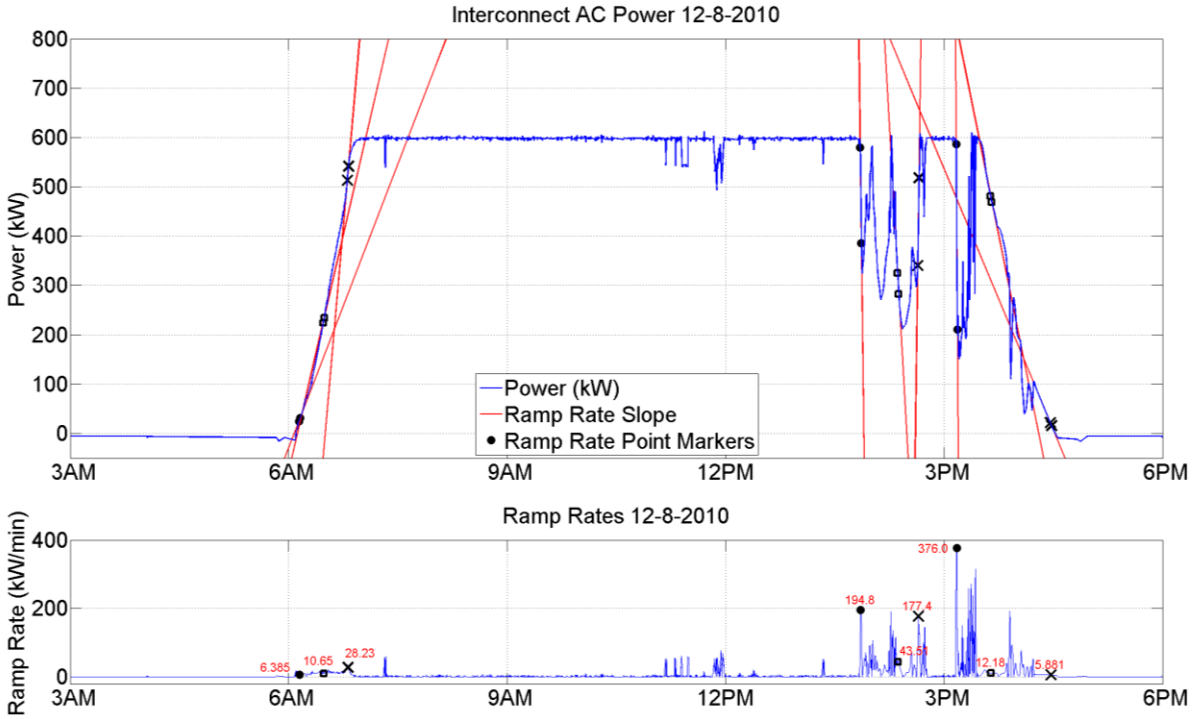

Figure 6. Graphical representation of nine 1-minute ramp rates during one sample day.

A histogram of 1-minute ramp rates December 7 and 8, 2010, is shown in Figure 7. Most of the morning and afternoon ramp rates fall within the 11 to 15 kW/min bin, which explains the spike in the histogram.

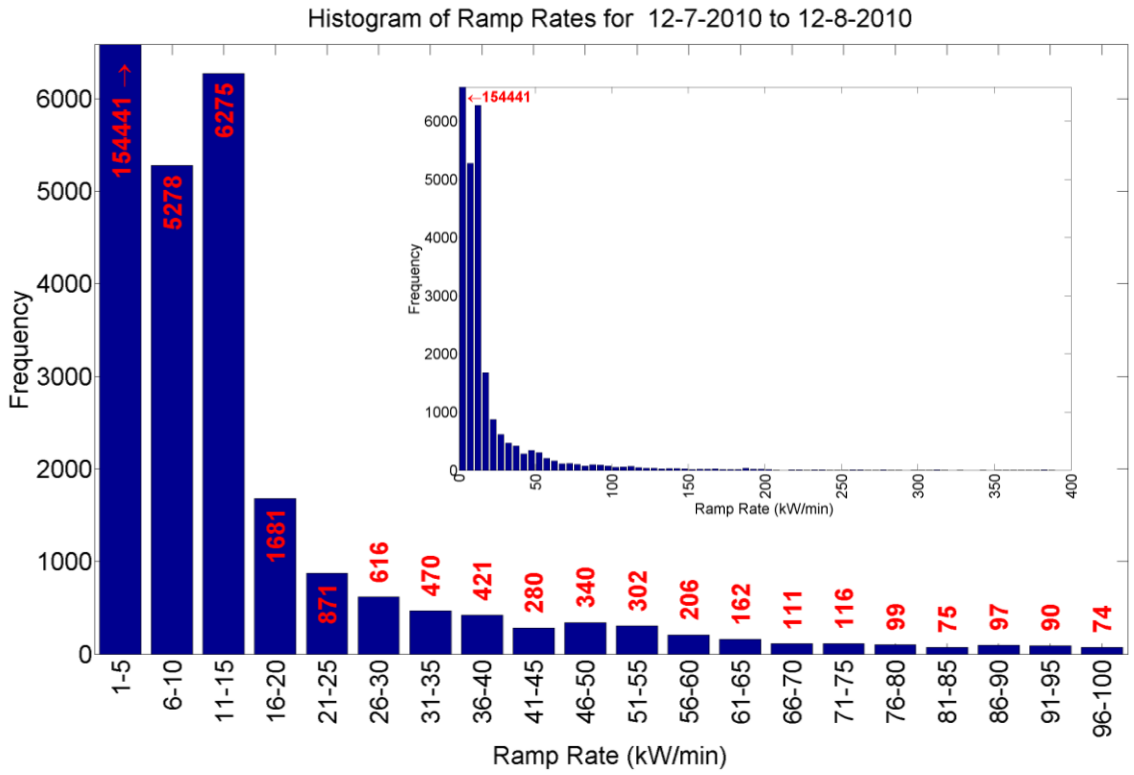

Figure 7. Histogram of 1-minute ramp rates for a 48-hour period (December 7 and 8, 2010).

For the purposes of this report, 1-minute ramp rates were defined as the absolute value of the difference between the instantaneous power at the beginning and at the end of a 1-minute period. It should be noted that ramp rate values are highly dependent on the time range used to determine the scalar ramp rate value. The 1-second ramp rates are far different than the 10-minute ramp rate. Formally, ramp rates over different time scales (Δt) can be calculated using the equation

$$Ramp\,Rate = \left| \frac{P(t_0) - P(t_0 + \Delta t)}{\Delta t} \right| \qquad \text{Eq. (1)}$$

where $P(t)$ is the time history of AC interconnect power provided to the grid with measurements taken at t in seconds, and Δt is the time interval. To illustrate the effect of time window, Table 1 shows maximum ramp rates calculated for 1-second, 10-second, 1-minute, and 10-minute time intervals for December 8, 2010.

Table 1. Maximum ramp rate for December 8, 2010 over different time windows.

Interval Δt	*Max Power Change (kW/Δt)*
1 second	49 kW/1 sec
10 seconds	194 kW/10 sec
1 minute	376 kW/1 min
10 minutes	454 kW/10 min

Figure 8 shows the CDFs of 1-second, 10-second, 1-minute, and 10-minute ramp rates in 2010. The annual results excluded 28 days with data or sensor errors. This type of data representation is more useful than the data shown in Table 1 because it represents the ramp rate distribution for the entire year. Note that 5% of 1-minute ramps are above 66.1 kW/min, 1% of 1-minute ramps are above 184.0 kW/min, and only 0.07% of 1-minute ramps are above 350.0 kW/min. The statistical results are based on 1-second data, and include daytime and nighttime periods. These results can be compared with the performance benchmark established for the Lanai PV/battery system (maximum 1-minute ramp rates limited to 360 kW/min).

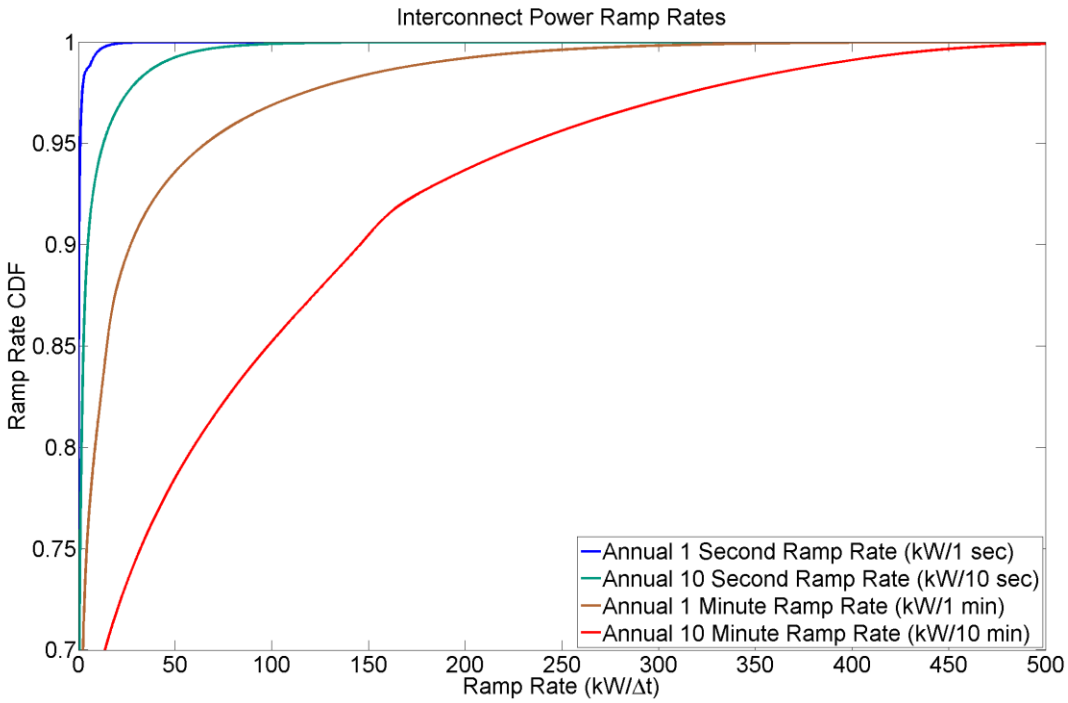

Figure 8. CDF of ramp rates for different Δt values for 2010.

The CDFs of 1-second, 10-second, 1-minute, and 10-minute ramp rates for variable (partly cloudy) conditions on November 4, 2010, clear conditions on December 7, 2010, and the 2010 annual ramp rates are shown in Figure 9. The variable day had larger ramp rates due to intermittent shading, so the ramp rates are larger than the 2010 average for each of the Δt values. Conversely, the clear day experienced fewer large ramp rate events, so the CDF is shifted to the left. In the 10-minute ramp rate plot, the clear day morning and evening ramp rates are shown

with the large number of samples between 100 and 150 kW/10 min. This matches closely with the 11-15 kW/min morning and evening ramp rates seen in Figures 6-7.

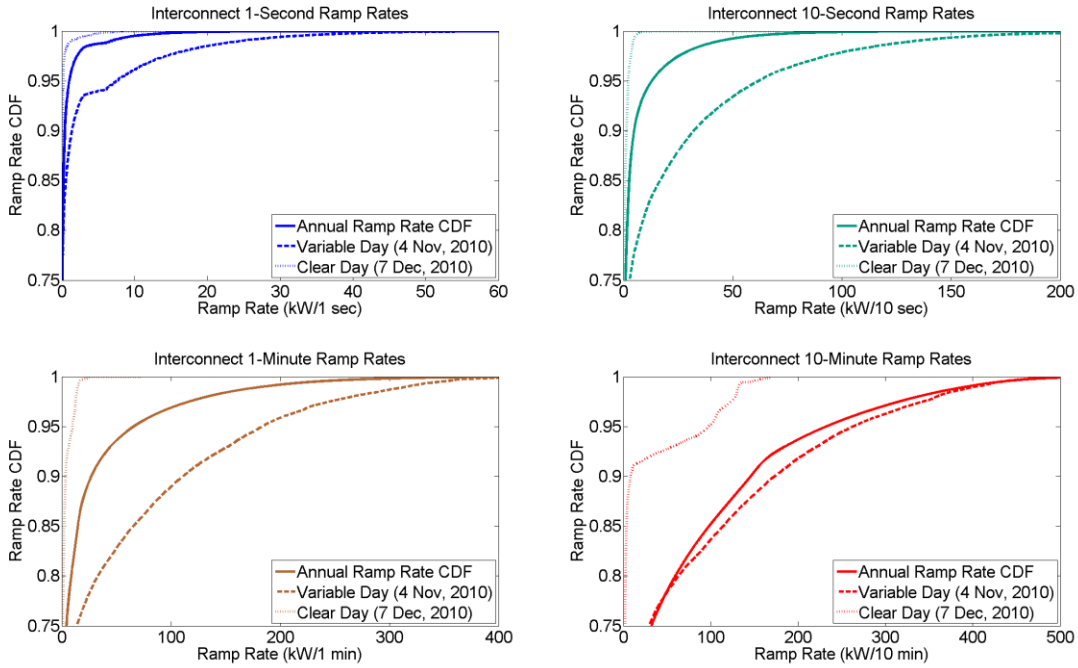

Figure 9. CDF of power change for different Δt values.

The AC power output profile and 99.5th percentile 1-minute ramp rate for first 8 days of each month of 2010 is shown in Figure 10. The number of times the ramp rate exceeded 200 kW/min is shown in Figure 11. It should be noted that the shorter the time interval, the more the ramp rate is influenced by signal noise and data communication delays. Thus, some of the high ramp rates are not due to irradiance variability. For example, an output drop can be seen in Figure 6, at approximately 7:30 AM, while irradiance measurements show a clear sky condition. To better represent the true high ramp rates and account for the effect of sensor noise, the ramp rates were calculated based on the 99.5th percentile. Highly variable days such as January 3 and 4, October 6, and November 4 experienced highest 1-minute ramp rates and largest number of events where the ramp rate exceeded 200 kW/min.

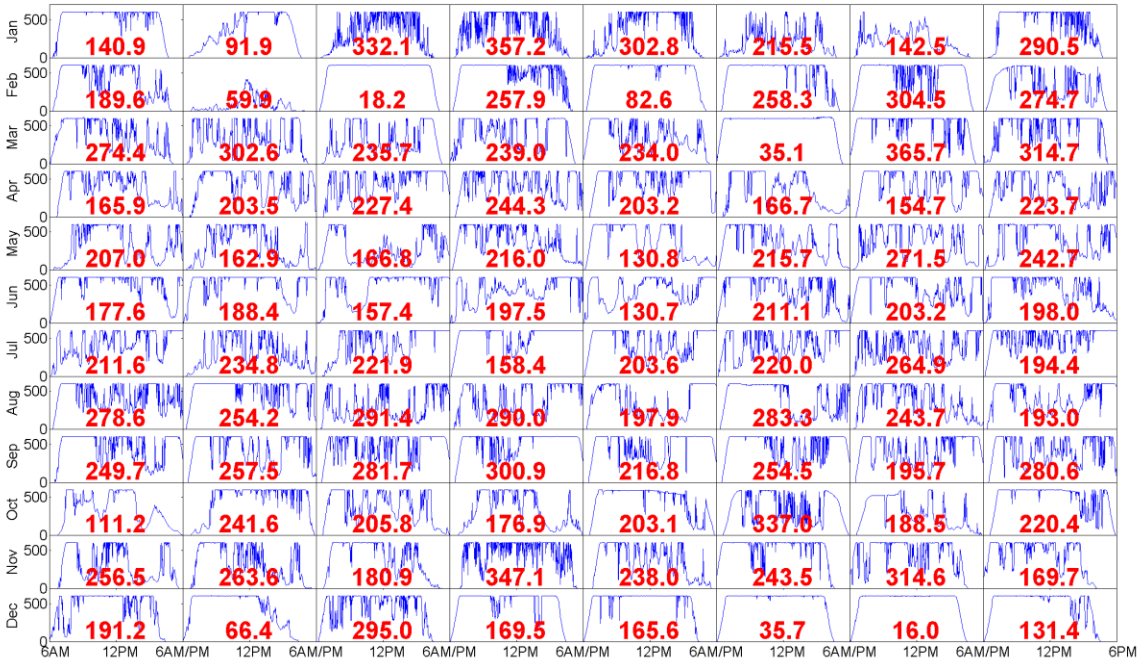

Figure 10. Power output profiles and the 99.5th percentile 1-minute ramp rates for 8 days at the beginning of each month in 2010.

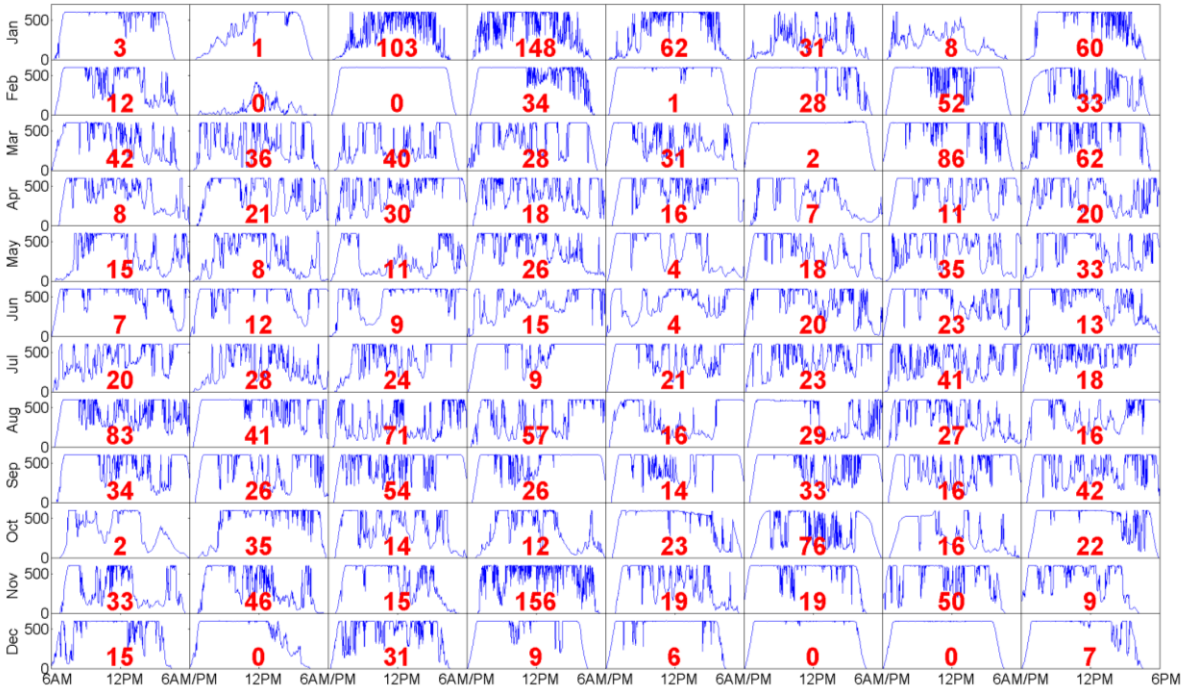

Figure 11. Number of incidents per day where the 1-minute ramp rate exceeded 200 kW/min.

The ramp rates in this report are an *instantaneous* or *windowed* power ramp rate metric, calculated based on the difference in interconnect power values separated by 60 seconds. Unfortunately, this method includes sub-minute variability contained in the 1-second samples. As shown above, ramp rates over short intervals are not always sustained over longer intervals, so normalizing them to a longer time basis may overstate the trend that the metric is intended to capture. Instead, calculating ramp rates based on the moving average or trend of the output power may be a more appropriate representation of variability over the timeframe of interest. One algorithm for determining an averaged ramp rate metric is taking the difference in means of X power values separated by Δt,

$$Ramp\ Rate_{averaged} = \left| \frac{\sum_{i=0}^{X-1} P(t_i) - \sum_{i=0}^{X-1} P(t_i + \Delta t)}{X\Delta t} \right| \qquad \text{Eq. (2)}$$

Averaging the data for one minute (X = 60) for 1-minute ramp rates (Δt = 60 seconds), the *averaged* ramp rates were calculated for each second in 2010. A comparison of instantaneous and averaged CDFs for a clear day, cloudy day, and all of 2010 is shown in Figure 12. For the clear day, since the ramps are due to long-term irradiance changes in the morning and evening, the two methods match very closely. The variable day, on the other hand, has large power ramps from short events as the clouds pass over the PV array. As a result, the averaged ramp rate reduces the magnitude of the ramps and there is a large difference in the two techniques. The annual result shows averaged ramp rates slightly lower than the instantaneous, however, there is generally a good correlation between the two metrics.

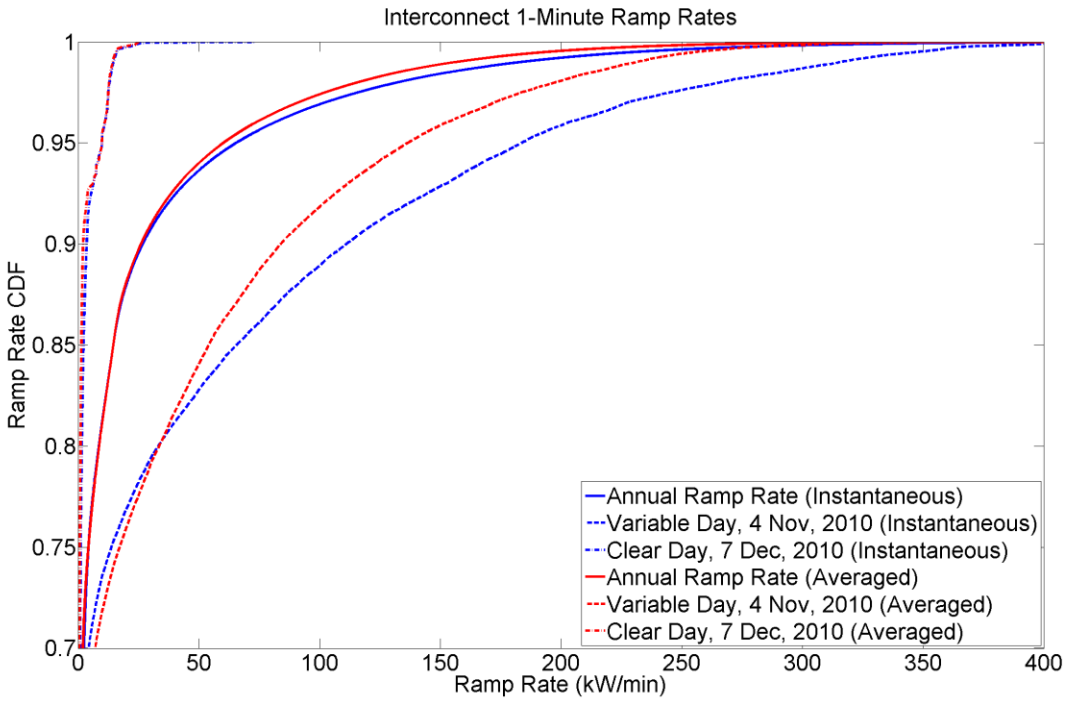

Figure 12. Comparison of instantaneous and averaged ramp rate calculation techniques.

2.3 Effect of Power Curtailment on Ramp Rates

During 2010 and thus far in 2011, the system power output was limited to 600 kW, or 50% of nameplate rating, to reduce large ramp rates. In order to understand the effect of power limiting on La Ola ramp rates under the same conditions, the spatial average of 12 POA irradiance sensors was used to predict the uncurtailed power. As discussed in Section 2.1, the spatial average of POA irradiance is roughly proportional to the power output. The estimated power output values were then limited to 600 kW and the ramp rates were compared with the ramp rates of the estimated un-curtailed power output. As shown in Figure 13, when the power is limited, the ramp rates are significantly reduced. Operation under 50% power limiting is shown by the purple trace. The blue and green traces show the one-minute ramp rates for the simulated full output and 50% output, respectively. The ramp rates discussed in this section were calculated with the *instantaneous* method as opposed to the *averaged* method.

For the December 1, 2010 sample data in Figure 13, maximum uncurtailed ramp rates are as high as 500 kW/min, while ramp rates with output limited to 50% of nameplate rating are less than 300 kW/min. Note that the large ramp rates between 1:40 PM and 1:55 PM have maximum 1-minute ramp rates for the uncurtailed PV system approximately twice as high as the curtailed output.

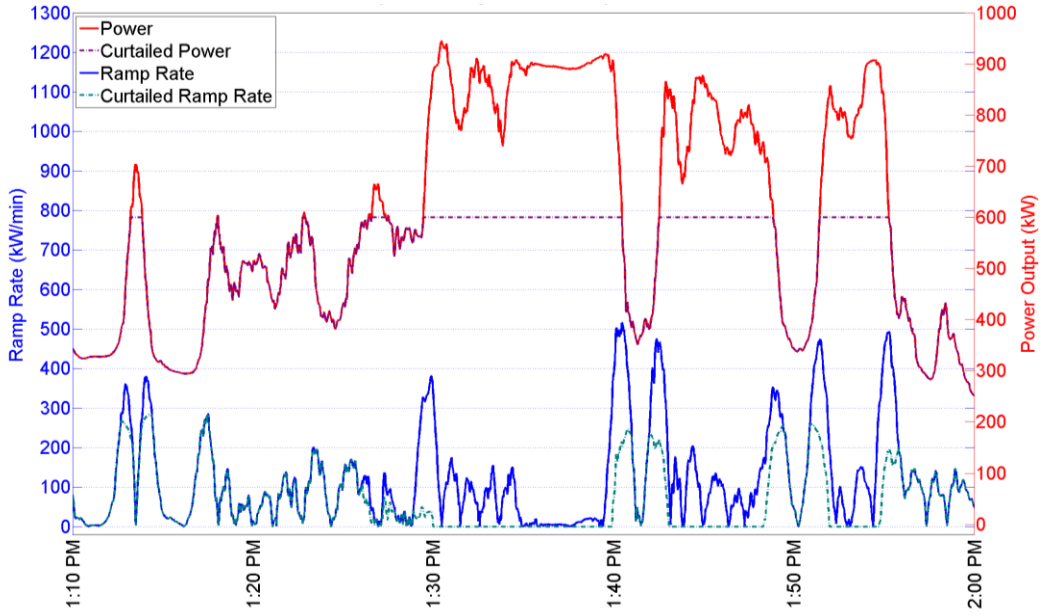

Figure 13. Example of reducing ramp rates by curtailing output power to 600 kW.

The annual estimated curtailed and uncurtailed 1-minute power ramp rates calculated from the spatially-averaged POA sensors are compared to the actual 1-minute power ramp rates in Figure 14. The estimated data does not include 44 days in 2010 with incomplete POA data. The results show the significant reduction in larger ramp rates due to curtailment, quantified in Table 2. For instance, 99% of the estimated ramp rates for the uncurtailed control routine are under 428.7 kW/min, whereas the bottom 99% of estimated curtailed ramp rates are below 221.0 kW/min. Based on values in Table 2, the curtailment control algorithm ramp rate appears to reduce the ramp rates by a factor of about 2.

The estimated curtailed 1-minute ramp rates closely approximate the actual 1-minute ramp rates observed during the same period of time (December 1, 2010). The differences are likely the result of two main factors: 1) the spatial averaging technique does not take into account secondary effects such as inverter response time, and 2) there are measurement errors in the POA irradiance as well as actual output data, which propagate trough the ramp rate calculation.

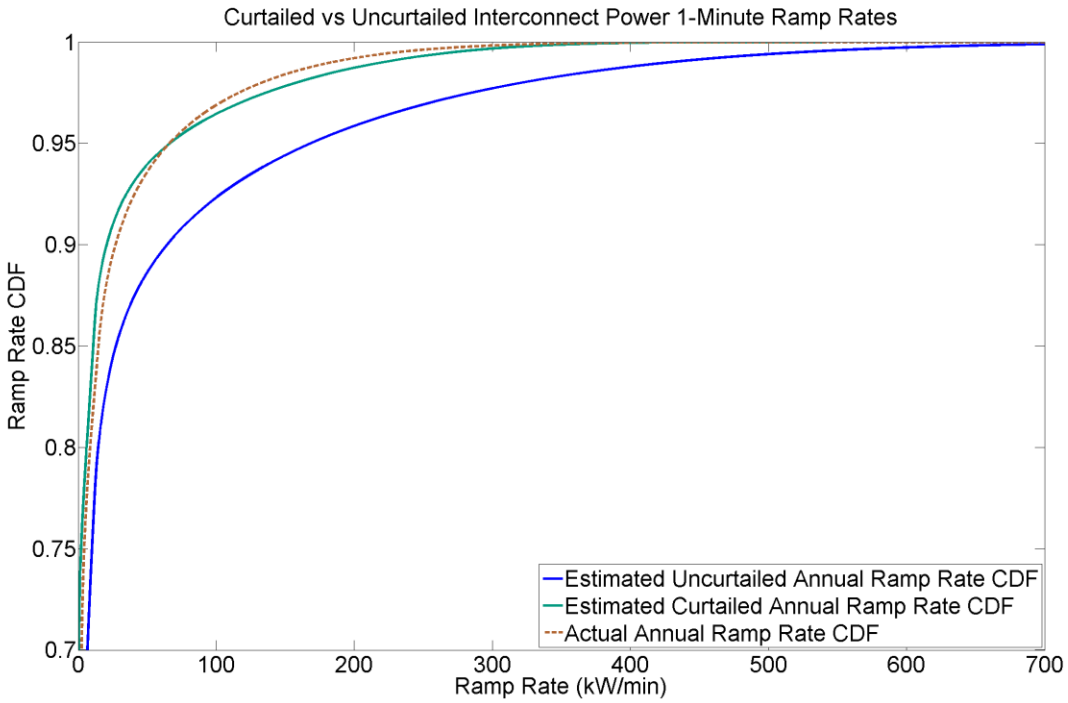

Figure 14. 2010 1-Minute Curtailed and Uncurtailed Ramp Rates.

Table 2. Curtailed vs. Uncurtailed 1-minute ramp rates values for different CDF values.

CDF percentage	*Estimated Uncurtailed Ramp Rate (kW/min)*	*Estimated Curtailed Ramp Rate (kW/min)*	*Actual Curtailed Ramp Rate (kW/min)*
80.0%	14.6	6.2	8.7
90.0%	64.4	20.7	27.1
95.0%	168.5	66.4	66.0
99.0%	428.7	220.0	184.1
99.5%	523.8	272.1	231.5
99.7%	587.3	304.4	265.7
99.9%	704.0	361.9	332.1

3. PV INFLUENCE ON THE LOCAL VOLTAGE AND GRID FREQUENCY

To measure the impact of power fluctuations on the Lanai grid, the frequency and voltage of the grid at the interconnection point were studied. It should be kept in mind that the data analyzed is at 1-second resolution and is time-synchronized. Only plant data was available for this analysis; therefore, impact of PV output variability on the nearby diesel generators was not characterized.[7]

3.1 Impact on Frequency

The frequency of the grid is an indication of generation and load imbalance. When the power demand exceeds the supply the frequency will tend to decrease from nominal level, and vice versa. Frequency deviations are counteracted by increased power output from the generators due to generator governor action. Grid operators ensure that online generators have sufficient maneuvering room up or down (spinning reserves) to follow net load fluctuations. When the headroom is insufficient, it may be necessary to turn off or turn on generating units. The existing diesel generators in Lanai are operated in this manner. Sometimes the online reserve may be insufficient to maintain system stability after a major contingency. To cover for the loss of a large generator outage, a frequency load-shedding scheme is implemented. The first load-shedding stage consists of turning off well pumps when frequency reaches 58.5 Hz. The primary concern used to justify the PV plant operating limit is the possibility that high PV plant ramps would cause system frequency to drop to this load-shedding threshold.

Analyses were performed to determine if the PV plant output ramp rates have had a noticeable effect on the frequency of the Lanai electrical system. Figures 15 and 16 show system frequency and PV plant output for two different days with output limited to 600 kW. During the first sample day PV output during the first sample day (November 4, 2010) is much more variable than during the second sample day (December 8, 2010).

[7] The Lanai diesel generators have active speed governors and voltage regulators to control system frequency and voltage.

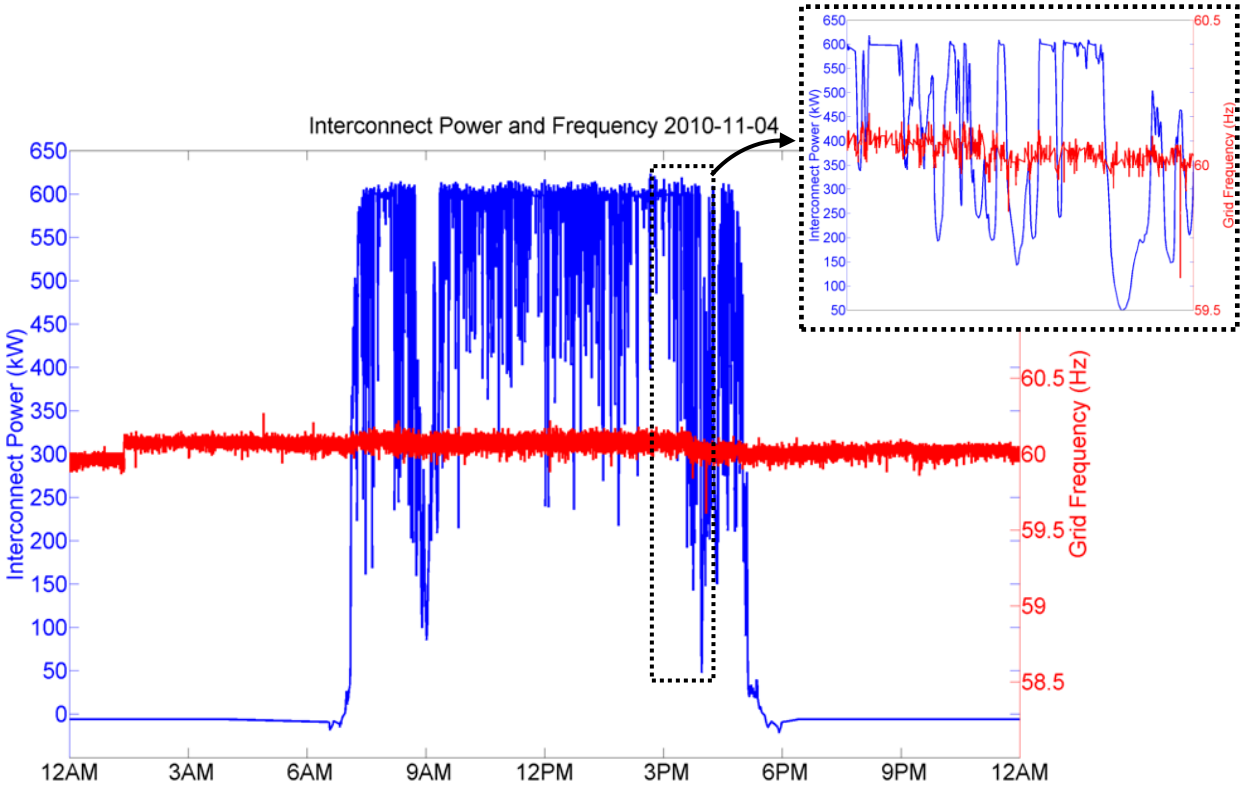

Figure 15. Real power versus frequency for November 4, 2010.

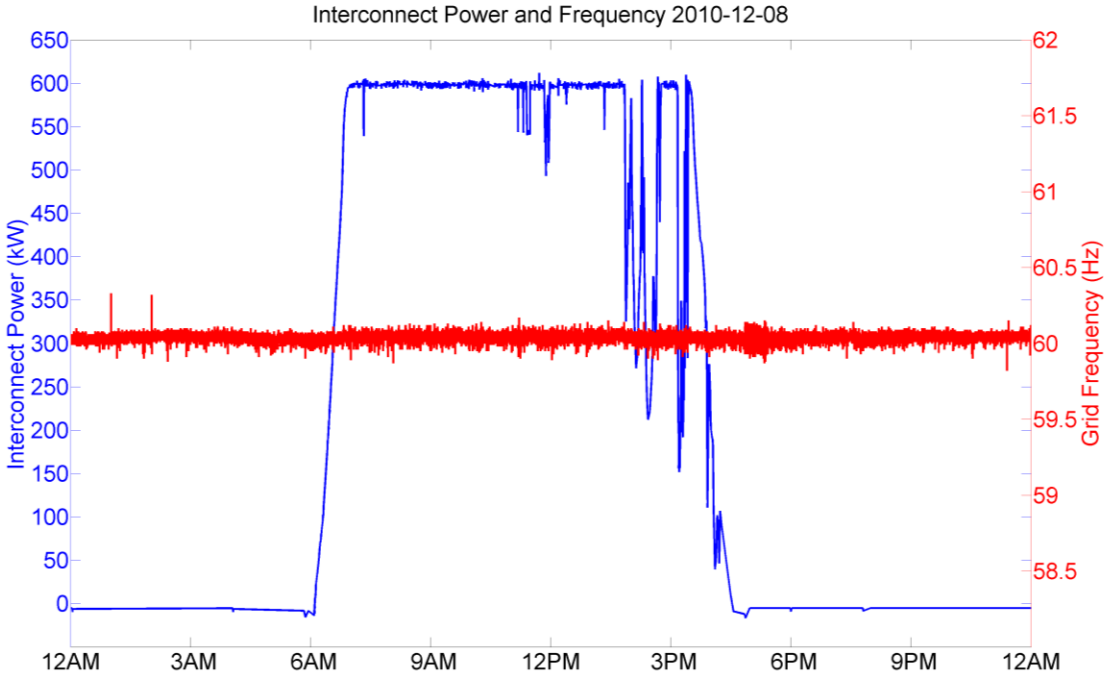

Figure 16. Real power versus frequency for December 8, 2010.

As shown in these figures, there is no significant change in the grid frequency in either day due to the morning/afternoon ramps, or due to PV output variability. In fact, the system frequency spread during the day is about the same as during the night, roughly 60.0 ±0.1 Hz. During these particular days, the lowest frequency measured was 59.6 Hz and the highest was 60.3 Hz. The largest change in frequency observed on November 4 was not related to a drop in PV output as, shown in the inset in Figure 15.

High-resolution data from the generating plant was unavailable to determine the extent to which the generators are working harder to "follow" the PV output variability in an effort to maintain frequency. However, the analysis shown above does indicate that the Lanai system frequency has not been materially impacted by the PV system with output limited to 600 kW.

3.2 Impact on Voltage

The PV inverters used at the La Ola site have the capability of absorbing and injecting reactive power. This reactive power capability could be used to dynamically compensate for the effect of variable PV output on local voltage, or to support steady-state feeder voltage. However, the plant does not directly control voltage; it is operated at a fixed power factor set-point issued by the grid operator. Typically, the power factor set-point is unity, meaning that the PV system reactive output is near zero. Therefore, to the extent that the PV plant causes voltage to change and the PV inverters are operated in constant power factor mode, the diesel generators would have to adjust reactive power output to compensate.

An analysis was performed to determine if the PV plant generation had any effect on the system voltage. Figures 17 and 18 show the real power produced by the PV plant and the line-to-ground root-mean-square (RMS) voltages at the point of common coupling (PCC) on November 4 and December 8, 2010.

The nominal RMS line-to-ground voltage for the system is 7.2 kV (12.47 kV line-line) and the voltage seen at the PCC is around 7.4 kV for all three phases. On a per-unit scale, the voltage level is 1.03 pu. The voltages remain within a narrow envelope even as PV power varies during the day. A slight effect on voltage level can be discerned during periods of sustained ramps, including morning and afternoon. Generally, however, the diurnal voltage profile is not significantly different from the nocturnal voltage profile, despite the relatively large PV power output swings. The reason for the relatively low impact on voltage is the fact that the PV plant is located close to the power plant, where voltage is actively regulated by the diesel generators. Generator reactive power output data was not available for this analysis.

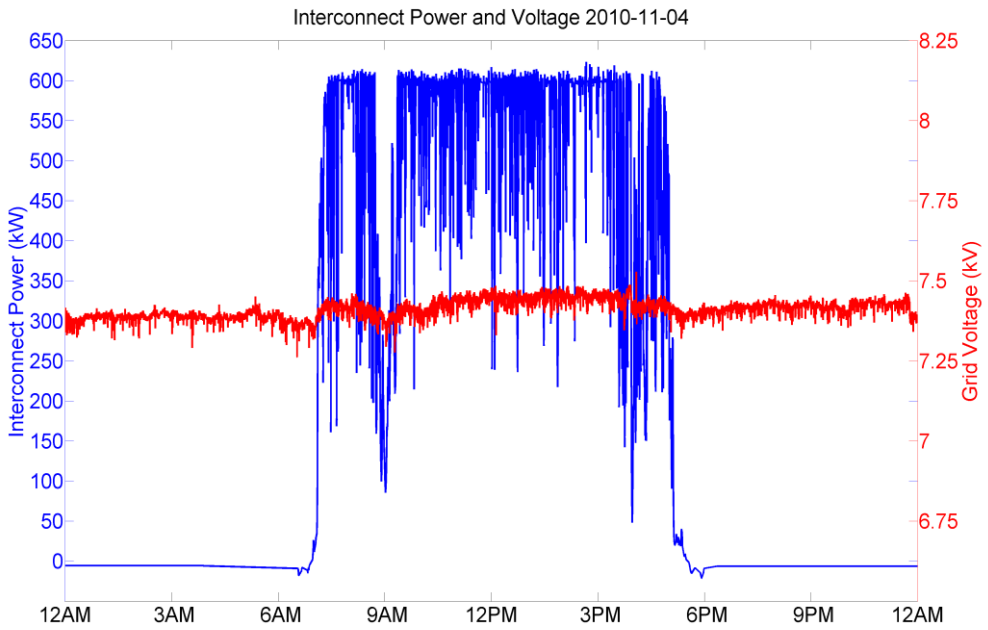

Figure 17. PV plant real power and phase line-to-ground RMS voltage for November 4, 2010.

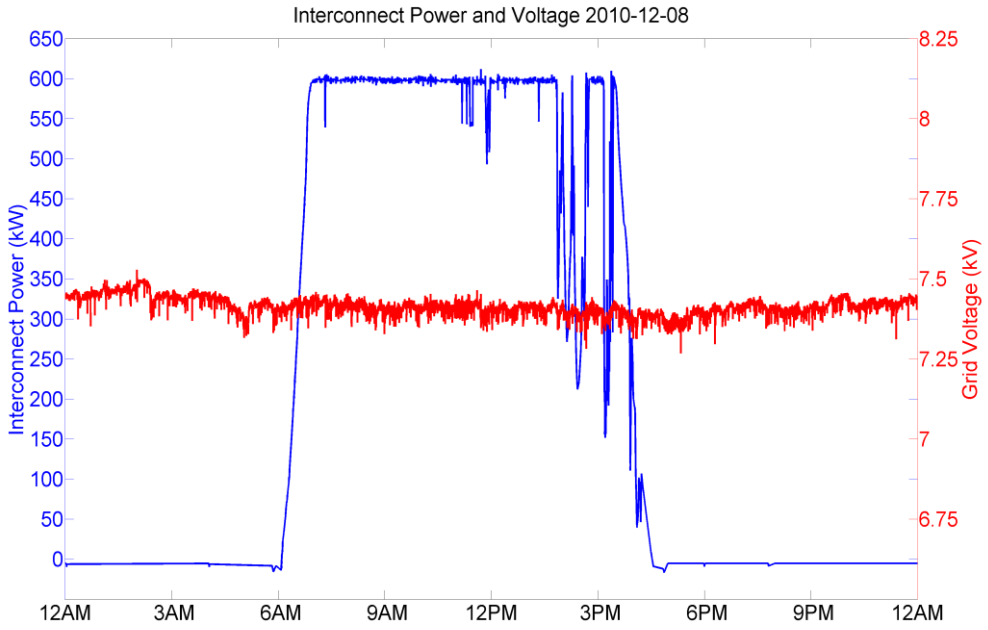

Figure 18. PV plant real power and phase line-to-ground RMS voltage for December 8, 2010.

4. IMPLICATIONS FOR ENERGY STORAGE OPERATION

A battery system was installed in summer 2011 to reduce power output variability with the plant operating at full power (1.2 MW). At the time this report was written, the energy storage system had not been fully commissioned; therefore, data on operational experience was unavailable for analysis. Nominally, the energy storage system is 1.125 MW, and has a capacity of 500 kWh.

Figure 19 illustrates the concept behind a very simple battery-based ramp rate control where the objective is to have a smoothed net output follow the moving average or trend of the PV output. In this example, the objective for the energy storage system is to remove high-frequency components of PV output such that the net output follows the trend (blue trace).

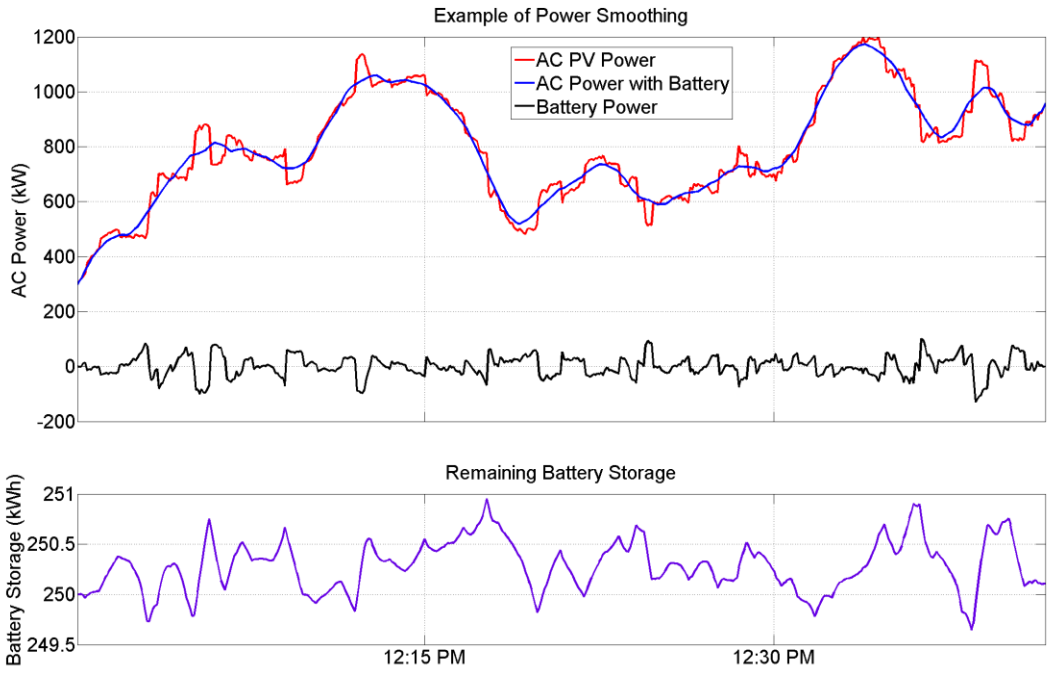

Figure 19. Example of ramp rate control for short time scales.

The degree of smoothing can be adjusted to suit the application. Figure 20 shows the same control approach as in Figure 19, but with a more aggressive, longer smoothing time constant. The disadvantage of using a longer smoothing time constant is that it would utilize more of the battery storage capacity, as can be seen by comparing the bottom half of the figures.

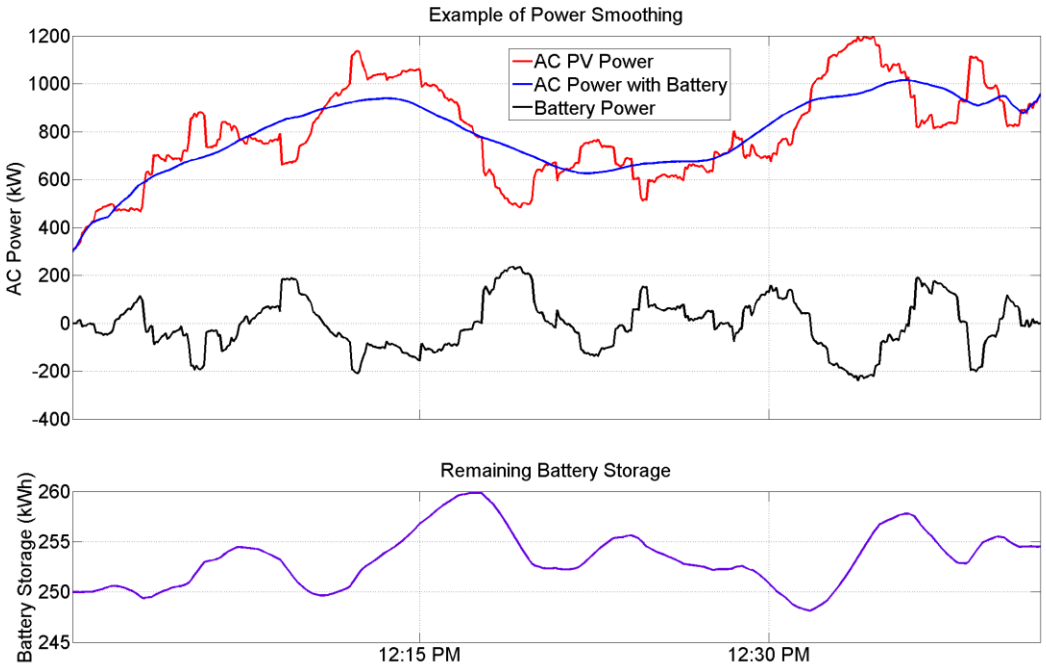

Figure 20. Example of ramp rate control for long time scales.

In the examples above, the target PV output trends (blue traces) are represented by an ideal moving average calculation. In a practical implementation, the target trends rely more heavily on past measurements. This means that the process of constructing the reference signal introduces a control time lag, with a more aggressive smoothing generally resulting is a larger time lag. This control lag can be reduced by making use of short-term output forecasting or similar techniques. Some time lag is not necessarily objectionable from the system point of view; however, a large lag would make the smoothing operation less efficient; that is, a larger portion of the energy storage capacity is utilized to achieve the same reduction in ramp rates. As mentioned before, other, more sophisticated smoothing strategies could be implemented. For example, a control algorithm could be designed strictly to reduce ramp rates to meet a certain performance criteria. This means that the energy storage will respond only large ramps when they approach a certain level. For example, the performance requirement for the La Ola PV system is that ramp rate of the net output should not be larger than 360 kW per minute, meaning that smaller ramp events need not be mitigated. This mode of operation might extend the battery life because it greatly reduces the charge/discharge activity. An example of such a control approach is shown in Figure 21 and 22 for 1-minute data. As shown in the figures, the battery is unused for the vast majority of the day and only becomes operational when the ramp rate becomes sufficiently large. A key concept is that this ramp rate threshold applies to 1-minute ramps. As shown in Figure 12, the number of ramp events during a variable output day is highly dependent on how the 1-minute ramp rate is calculated. However, independent of the method of calculating the ramp rate, the energy storage shown in Figures 21 and 22 could mitigate 1-minute ramp rates above 360 kW/minute.

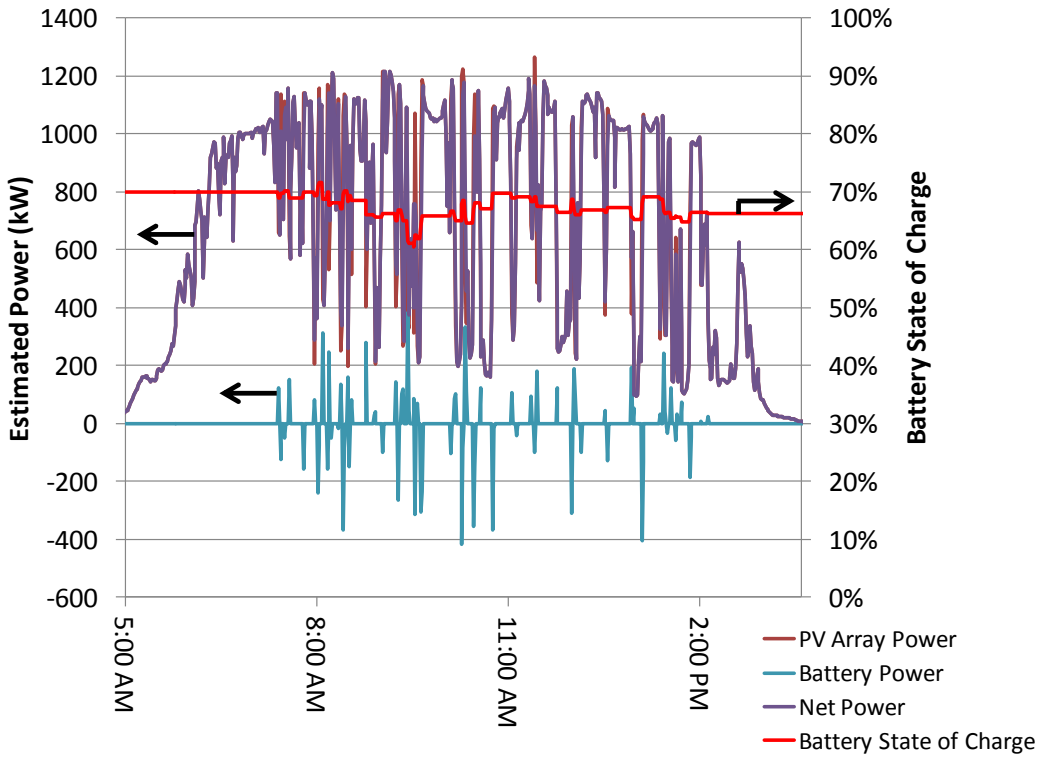

Figure 21. A ramp rate mitigating control algorithm which avoids heavy battery use.

Figure 22. A closer view of the control algorithm mitigating large ramp rates.

5. CONCLUSIONS

High-resolution data for the La Ola PV power plant was analyzed. During the analysis period, the system output was limited to 50% of nominal AC rating, or 600 kW. The operating limitation was established due to concerns that high output variability could materially impact voltage and frequency on the small Lanai island host grid. Under output-limited operating conditions, observed PV output 1-minute ramp rates were commonly above 200 kW/min, and maximum observed 1-minute ramp rates were on the order of 380 kW/min. Despite the high ramp rates, PV plant operation has as not had a significant negative impact on voltage and frequency as measured at the PCC. The diesel generators at the nearby power station regulate voltage and frequency, and the degree to which their operation has been impacted by PV system variability was not analyzed due unavailability of high-resolution data. It is estimated that, without the existing output limitation of 50%, maximum 1-minute ramp rates for PV output could be higher by a factor of 2. Recently, an energy storage system was deployed at the PV plant. When fully commissioned, the energy storage system will be used to reduce net output ramp rates and thus allow the PV plant to operate without output limitation.

DISTRIBUTION

3 U.S. Department of Energy
Solar Energy Technology Program
Attn: Kevin Lynn
Alvin Razon
Jennifer DeCesaro
950 L'Enfant Plaza
Washington, DC 20585

1 U.S. Department of Energy
Attn: Dan T. Ton
1000 Independence Ave. SW
EE-2A, FORS
Washington, DC 20585

1 U.S. Department of Energy/ALO
Attn: Dan Sanchez
Pennsylvania & H Street
Kirtland AFB, NZ-384-3
Albuquerque, NM 87184

1 UWIG
Attn: Charlie Smith
Utility Wind Integration Group
P.O. Box 2787
Reston, VA 20195

2 EPRI
Attn: Tom Key
Daniel Brooks
942 Corridor Park Blvd.
Knoxville, TN 37932

2 National Renewable Energy Laboratory
Attn: Brian Parson
Benjamin Kroposki
1617 Cole Blvd.
Golden, CO 80401-3305

1 Solar Electric Power Association
Attn: Julia Hamm, Executive Director
1220 19th St., Suite 401
Washington, DC 33708

1 SunPower Corporation
Attn: Carl Lenox
William Peter
1414 Harbour Way South
Richmond, CA 94804

1	MS0321	Robert W. Leland	01400
1	MS0321	John L. Mitchiner	01460
1	MS0352	Jay Johnson	01718
1	MS0352	W. Kent Schubert	01718
1	MS0721	Marjorie L. Tatro	06100
1	MS0734	Ward I. Bower	06111
1	MS1033	Stanley Atcitty	06113
3	MS1033	Abraham Ellis	06112
1	MS1033	Jennifer E. Granata	06112
1	MS1033	Charles J. Hanley	06112
1	MS1033	Jimmy Quiroz	06112
1	MS1078	Wahid L. Hermina	01710
1	MS1079	Gilbert V. Herrera	01700
1	MS1082	Anthony L. Lentine	01727
1	MS1104	Rush D. Robinett III	06110
1	MS1108	Ross Guttromson	06113
1	MS1108	Benjamin L. Schenkman	06113
1	MS1108	Juan J. Torres	06111
1	MS1318	Bruce A. Hendrickson	01440
1	MS1318	Robert J. Hoekstra	01426
1	MS1321	David A. Schoenwald	01444
1	MS1321	Randall M. Summers	01444
1	MS1322	Sudip S. Dosanjh	01420

1	MS0359	D. Chavez, LDRD Office	01911
1	MS0899	RIM-Reports Management	09532 *(electronic copy)*


Sandia National Laboratories